Supplement of

SO_2 and NH_3 emissions enhance organosulfur compounds and fine particles formation from the photooxidation of a typical aromatic hydrocarbon

Zhaomin Yang et al.

Correspondence to: Lin Du (lindu@sdu.edu.cn)

Table S1. Summary of characteristic wavenumbers of selected functional groups.

Functional groups	Absorption frequencies (cm^{-1})	References
organic nitrates ($RONO_2$)	860, 1280, 1630–1640	(Bruns et al., 2010)
sulfates (SO_4^{2-})	612–615, 1103–1135	(Hawkins et al., 2010)
aliphatic carbon (C-H)	2850–3000	(Zhong and Jang, 2014)
esters (RC(O)OR’)	1050–1160	(Hung et al., 2013)
O-O	960	(Jia and Xu, 2018)
C-N stretch	1315	(Liu et al., 2015)
carboxylic acids (RC(O)OH)	875–970, 1210–1320, 1685–1740, 2500–3300	(Hung et al., 2013)
aldehydes (RC(O)H)	1325–1450, 1720–1740	(Hung et al., 2013)
ketones (RC(O)R’)	1100–1170, 1715–1745	(Hung et al., 2013)
alcohols (R-OH)	3200–3500	(Zhong and Jang, 2014)

Table S2. Organosulfur compounds detected in aerosol particles from TMB/NO_x/SO_2 photooxidation using UPLC-HRMS.

Molecular weight	Measured $[M - H]^-$	Suggested ion formula	Error (ppm) [a]	Proposed chemical structure
Organosulfates				
226	225.00772	$C_6H_9O_7S^-$	1.219	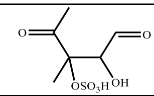
228	227.00150	$C_5H_7O_8S^-$	-2.059	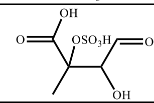
240	239.02271	$C_7H_{11}O_7S^-$	-1.638	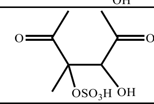
242	241.00168	$C_6H_9O_8S^-$	-2.833	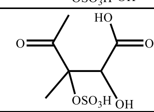
244	242.99619	$C_5H_7O_9S^-$	-2.886	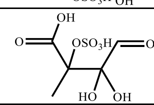
300	299.04395	$C_9H_{15}O_9S^-$	-0.938	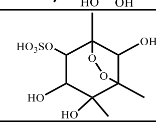
316	315.03867	$C_9H_{15}O_{10}S^-$	-1.494	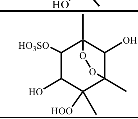
345	344.02853	$C_9H_{14}O_{11}NS^-$	-2.250	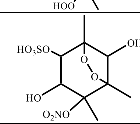
214	212.98590	$C_8H_5O_5S^-$	-1.954	Unidentified
268	267.01724	$C_8H_{11}O_8S^-$	-2.879	Unidentified
Organic sulfonates				
228	227.00159	$C_9H_7O_5S^-$	-1.675	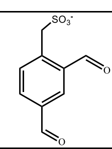
230	229.01706	$C_9H_9O_5S^-$	-2.437	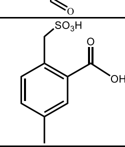

[a] The molecular formula was assigned based on accurate mass measurements with a mass tolerance of ± 5 ppm.

Table S3. Observed products in NH_3-involved photooxidation.

Molecular weight	Measured ions	Suggested ion formula	Error (ppm) [c]	O/C	$\log_{10}C^*$ ($\mu g\ m^{-3}$) [d]
74 [a]	72.99308	$C_2HO_3^-$	-0.508	1.50	6.16
88 [a]	87.00876	$C_3H_3O_3^-$	-0.100	1.00	6.18
150 [a]	149.0088	$C_4H_5O_6^-$	-1.882	1.50	2.16
114 [a]	113.02439	$C_5H_5O_3^-$	-0.231	0.60	5.87
146 [a]	145.01407	$C_5H_5O_5^-$	-1.277	1.00	3.53
162 [a]	161.00876	$C_5H_5O_6^-$	4.311	1.20	2.23
148 [a]	147.02985	$C_5H_7O_5^-$	-0.342	1.00	3.53
164 [a]	163.02470	$C_5H_7O_6^-$	-0.657	1.20	2.23
174 [a]	173.00879	$C_6H_5O_6^-$	4.188	1.00	2.20
128 [a]	127.04013	$C_6H_7O_3^-$	0.497	0.50	5.61
144 [a]	143.03482	$C_6H_7O_4^-$	-1.128	0.67	4.58
160 [a]	159.03011	$C_6H_7O_5^-$	1.314	0.83	3.43
176	175.02451	$C_6H_7O_6^-$	4.520	1.00	2.20
146 [a]	145.05052	$C_6H_9O_4^-$	-0.759	0.67	4.58
162 [a]	161.04543	$C_6H_9O_5^-$	-0.753	0.83	3.43
178 [a]	177.04028	$C_6H_9O_6^-$	-1.005	1.00	2.20
172 [a]	171.02988	$C_7H_7O_5^-$	-0.116	0.71	3.28
188 [a]	187.02446	$C_7H_7O_6^-$	3.985	0.86	2.11
156 [a]	157.05048	$C_7H_9O_4^-$	-0.993	0.57	4.36
174 [a]	173.04514	$C_7H_9O_5^-$	-2.376	0.71	3.28
190 [a]	189.03993	$C_7H_9O_6^-$	3.003	0.86	2.11
160 [a]	159.06609	$C_7H_{11}O_4^-$	-1.234	0.57	4.36
176 [a]	175.06070	$C_7H_{11}O_5$	-2.840	0.71	3.28
216 [a]	215.01923	$C_8H_7O_7^-$	-2.324	0.88	0.79
186 [a]	185.04509	$C_8H_9O_5^-$	-2.469	0.63	3.08
202 [a]	201.04025	$C_8H_9O_6^-$	4.418	0.75	1.97
188 [a]	187.06075	$C_8H_{11}O_5^-$	-2.413	0.63	3.08
204 [a]	203.05577	$C_8H_{11}O_6^-$	3.724	0.75	1.97
184 [b]	185.08040	$C_9H_{13}O_4^+$	-2.360	0.44	3.81
216 [a]	215.05579	$C_9H_{11}O_6^-$	-1.512	0.67	1.79
232 [a]	231.05043	$C_9H_{11}O_7^-$	2.169	0.78	0.66
264 [a]	263.03973	$C_9H_{11}O_9^-$	-4.262	1.00	-1.77
202	201.07658	$C_9H_{13}O_5^-$	-1.307	0.56	2.85

Table S3. Continued.

Molecular weight	Measured ions	Suggested ion formula	Error (ppm) [c]	O/C	$log_{10}C^*$ (μg m^{-3}) [d]
218 [a]	217.07117	$C_9H_{13}O_6^-$	2.314	0.67	1.79
234 [a]	233.06613	$C_9H_{13}O_7^-$	-2.336	0.78	0.66
250 [a]	249.06107	$C_9H_{13}O_8^-$	-2.107	0.89	-0.53
220 [a]	219.08690	$C_9H_{15}O_6^-$	-2.339	0.67	1.79
236 [a]	235.08188	$C_9H_{15}O_7^-$	-1.903	0.78	0.66
252 [a]	251.07664	$C_9H_{15}O_8^-$	-2.372	0.89	-0.53
229 [a]	228.05083	$C_9H_{10}O_6N^-$	-2.338	0.67	0.36
229 [b]	230.06591	$C_9H_{12}O_6N^+$	-3.365	0.67	0.36
231 [a]	230.06701	$C_9H_{12}O_6N^-$	-2.028	0.67	0.36
231 [b]	232.08087	$C_9H_{14}O_6N^+$	-2.981	0.67	0.36
265 [a]	264.07187	$C_9H_{14}O_8N^-$	-2.350	0.89	-1.09
265 [b]	266.08615	$C_9H_{16}O_8N^+$	-3.351	0.89	-1.09
191 [a]	190.03529	$C_6H_8O_6N^-$	-2.192	1.00	1.36

[a] The molecules were detected by UPLC-HRMS in the negative mode.

[b] The molecules were detected by UPLC-HRMS in the positive mode.

[c] The molecular formula was assigned based on accurate mass measurements with a mass tolerance of ± 5 ppm.

[d] The saturation mass concentrations of observed products were predicted based on the method of Li et al. (2016).

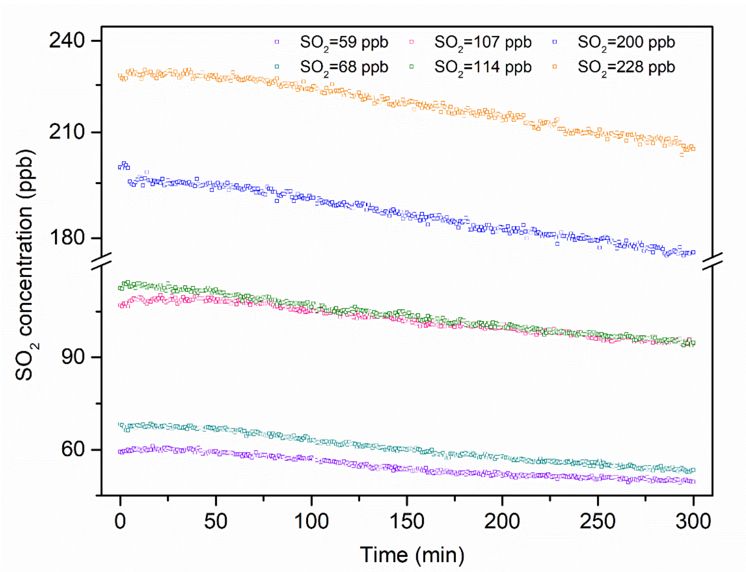

Figure S1. Decay of SO_2 during the photooxidation of TMB (Exps. 2–4, 6–8).

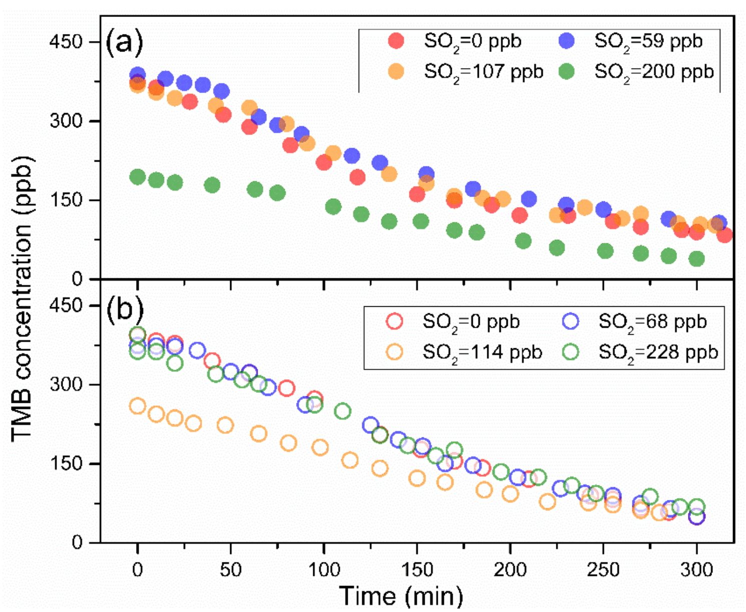

Figure S2. Time profiles of TMB for photooxidation experiments under low- (a) and high-NO_x (b) conditions with different SO_2 levels.

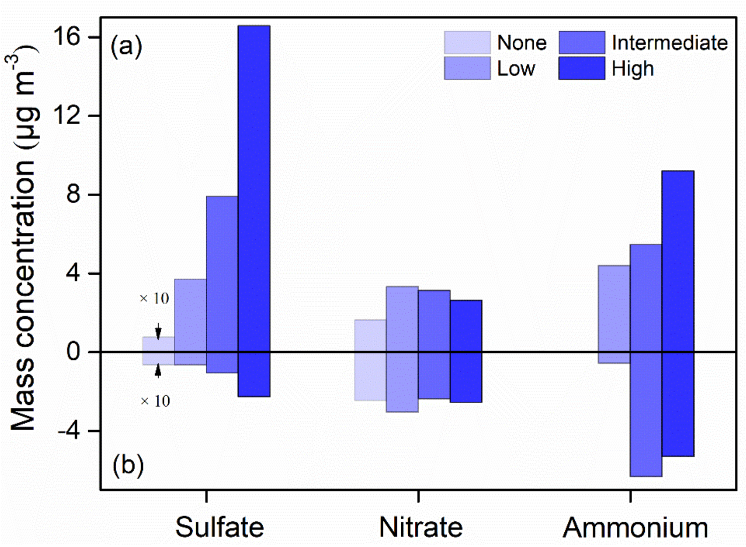

Figure S3. The particle sulfate, nitrate, and ammonium loadings for aerosol samples collected from the photooxidation of TMB under low- (a) and high-NO_x (b) conditions with SO_2 introduction. None: SO_2 = 0 ppb; low: SO_2 = 50–70 ppb intermediate: SO_2 = 100–120 ppb; high: SO_2 = 200–230 ppb.

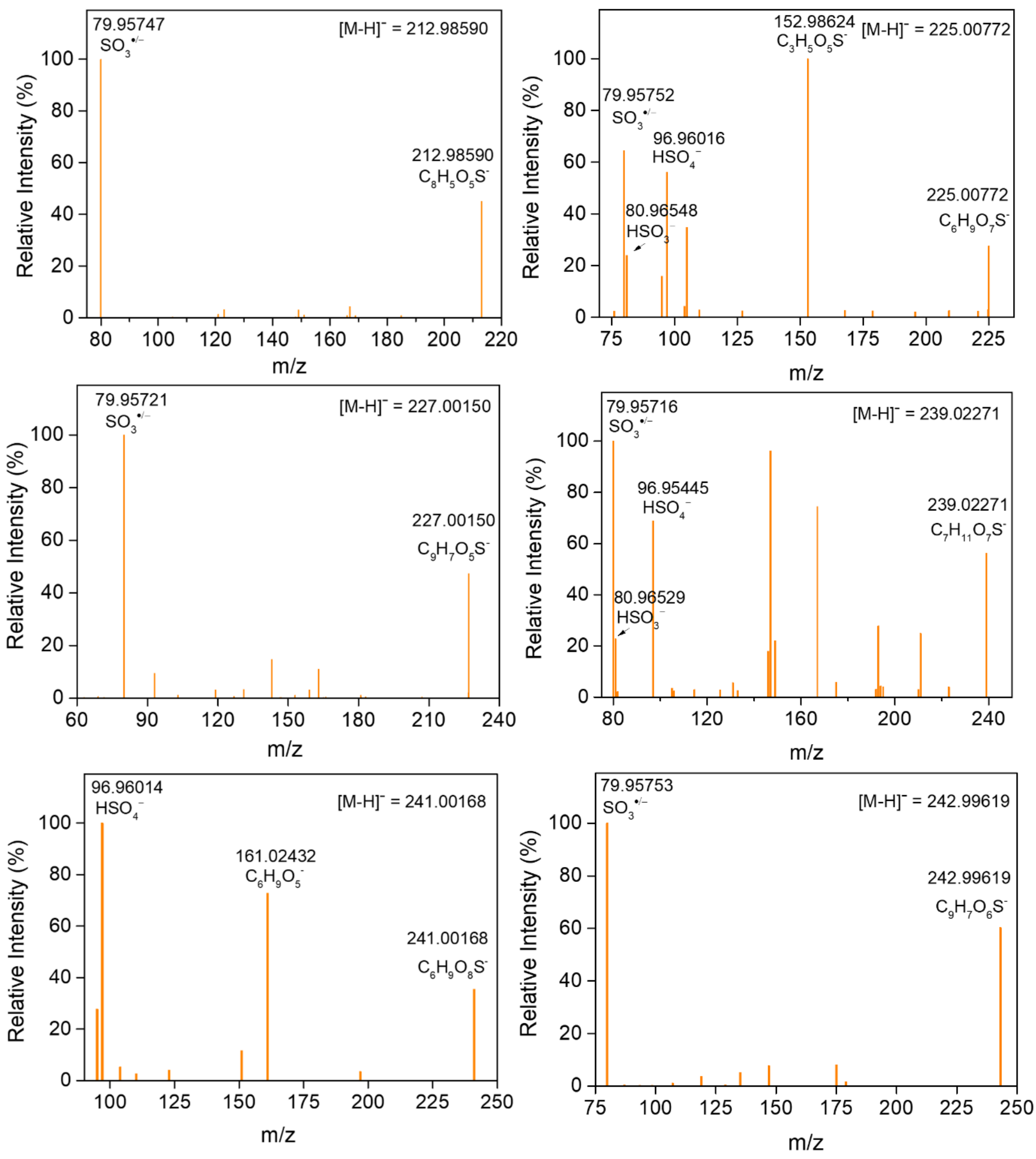

Figure S4. MS/MS spectra of organosulfates generated from the photooxidation of TMB in the presence of SO_2.

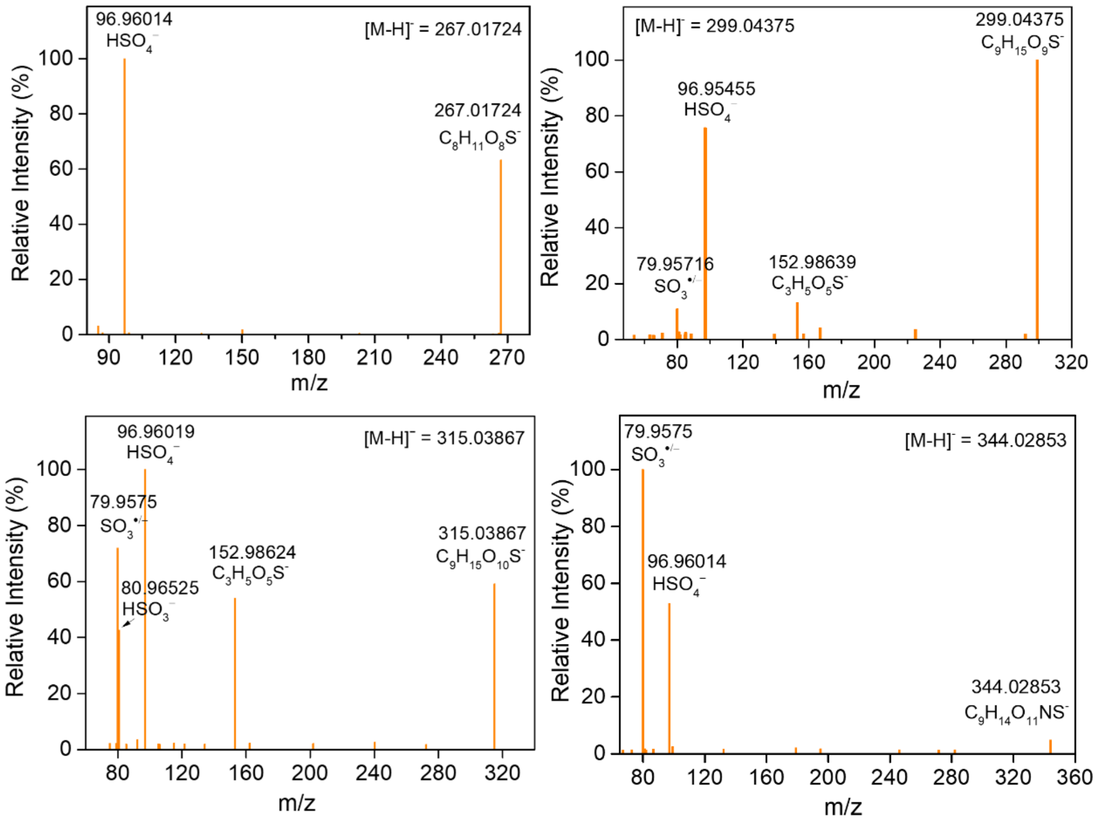

Figure S4. Continued.

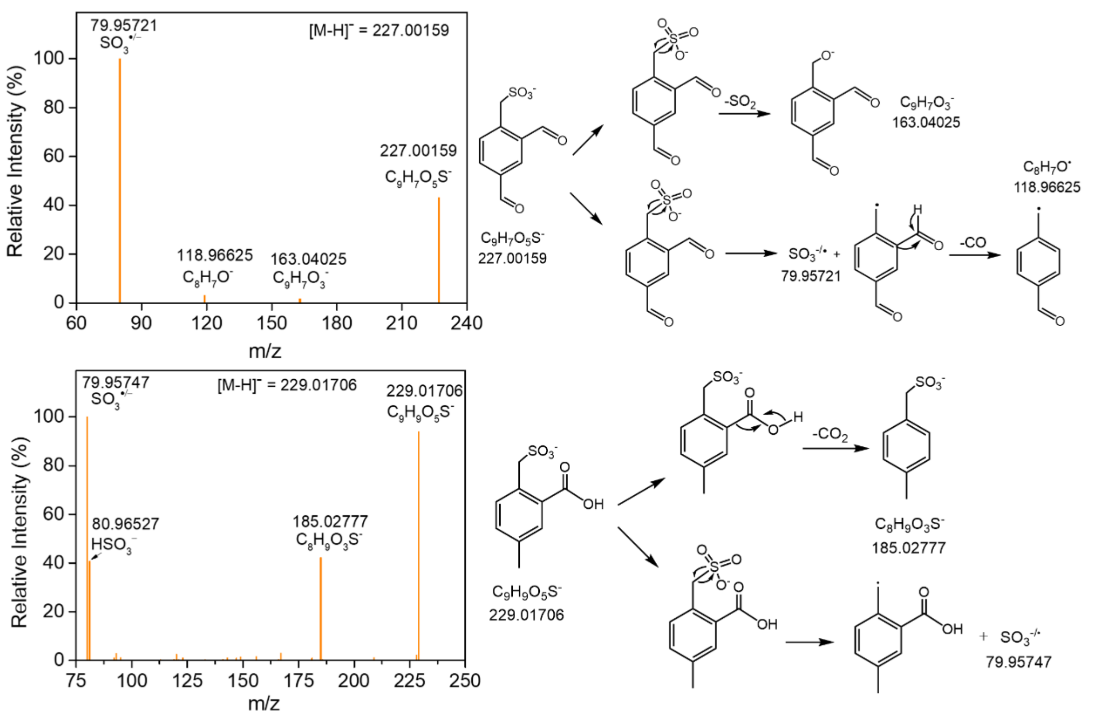

Figure S5. MS/MS spectra and fragmentation schemes of ion at m/z 227.00159 and 229.01706 observed in aerosol particles from TMB photooxidation in the presence of SO_2.

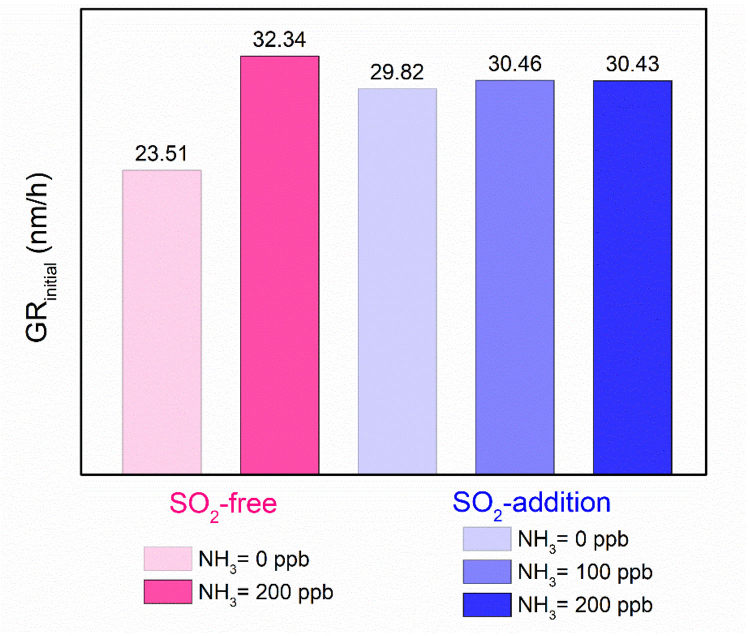

Figure S6. Observed initial growth rates of aerosol particles under SO_2-free and SO_2-added (~ 230 ppb) conditions (Exps. 5, 8, 10–12).

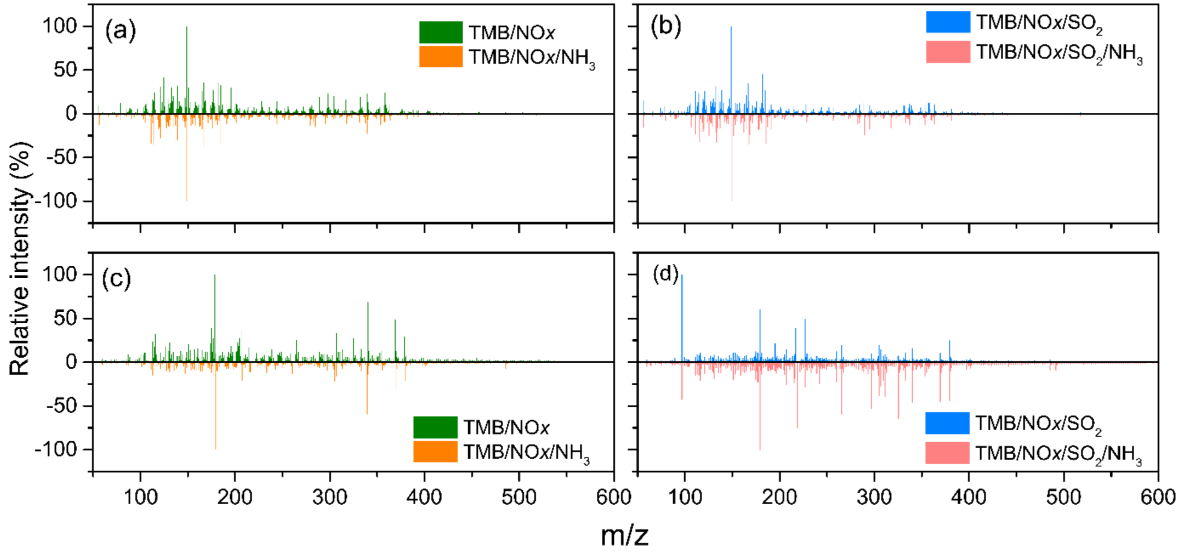

Figure S7. High-resolution mass spectra of aerosol particles from TMB photooxidation with/without NH_3 introduction. Panels a–b: positive ion mode. Panels c–d: negative ion mode.

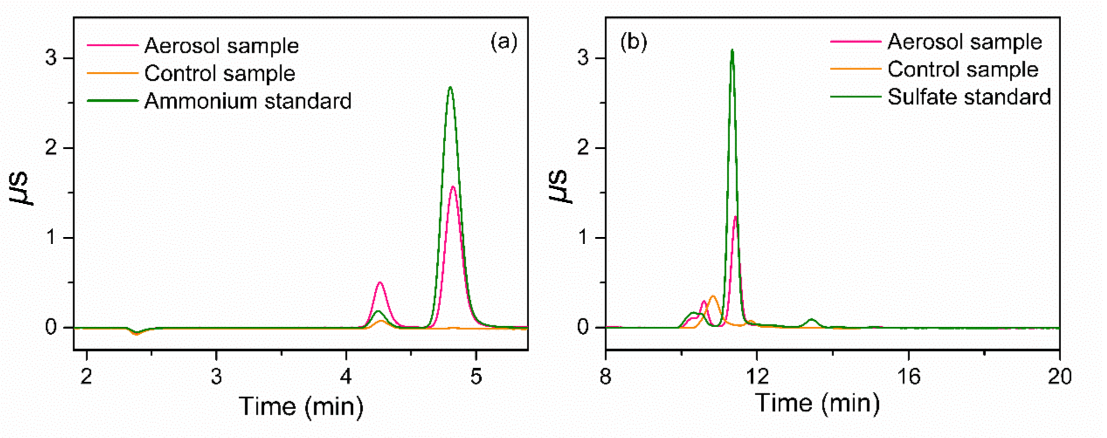

Figure S8. Ion chromatography results for aerosol particles formed from the photooxidation of TMB in the presence of SO_2 and NH_3. Panel (a): Ammonium. Panel (b): Sulfate.

References

Bruns, E. A., Perraud, V., Zelenyuk, A., Ezell, M. J., Johnson, S. N., Yu, Y., Imre, D., Finlayson-Pitts, B. J., and Alexander, M. L.: Comparison of FTIR and particle mass spectrometry for the measurement of particulate organic nitrates, Environ. Sci. Technol., 44, 1056-1061, 10.1021/es9029864, 2010.

Hawkins, L. N., Russell, L. M., Covert, D. S., Quinn, P. K., and Bates, T. S.: Carboxylic acids, sulfates, and organosulfates in processed continental organic aerosol over the southeast Pacific Ocean during VOCALS-REx 2008, J. Geophys. Res., 115, 10.1029/2009jd013276, 2010.

Hung, H. M., Chen, Y. Q., and Martin, S. T.: Reactive aging of films of secondary organic material studied by infrared spectroscopy, J. Phys. Chem. A, 117, 108-116, 10.1021/jp309470z, 2013.

Jia, L., and Xu, Y.: Different roles of water in secondary organic aerosol formation from toluene and isoprene, Atmos. Chem. Phys., 18, 8137-8154, 10.5194/acp-18-8137-2018, 2018.

Li, Y., Pöschl, U., and Shiraiwa, M.: Molecular corridors and parameterizations of volatility in the chemical evolution of organic aerosols, Atmos. Chem. Phys., 16, 3327-3344, 10.5194/acp-16-3327-2016, 2016.

Liu, Y., Liggio, J., Staebler, R., and Li, S. M.: Reactive uptake of ammonia to secondary organic aerosols: kinetics of organonitrogen formation, Atmos. Chem. Phys., 15, 13569-13584, 10.5194/acp-15-13569-2015, 2015.

Zhong, M., and Jang, M.: Dynamic light absorption of biomass-burning organic carbon photochemically aged under natural sunlight, Atmos. Chem. Phys., 14, 1517-1525, 10.5194/acp-14-1517-2014, 2014.